Retrieval of south Asian monsoon variation during the Holocene from natural climate archives

R. Ramesh[1,*], M. Tiwari[2], S. Chakraborty[3], S. R. Managave[1,5], M. G. Yadava[1] and D. K. Sinha[4]

[1]Geoscience Division, Physical Research Laboratory, Navrangpura, Ahmedabad 380 009, India
[2]National Centre for Antarctic and Ocean Research, Headland Sada, Vasco da Gama, Goa 403 804, India
[3]Indian Institute of Tropical Meteorology, Homi Bhabha Road, Pashan, Pune 410 007, India
[4]Department of Geology, Centre of Advanced Studies, University of Delhi, Delhi 110 007, India
[5]Present address: Department of Geology, Pondicherry University, Kalapet, Puducherry 605 014, India

We review the available reconstructions of the Indian summer and winter monsoons using well-dated natural climatic archives such as tree-rings, corals, ice-cores, speleothems and ocean sediments. Oxygen isotopic analyses of cellulose from annual growth rings of teak trees on an intra-annual scale hold high promise for reconstructing rainfall during both monsoons. Oxygen isotopic variations in corals and ice-cores seem to respond to atmospheric and ocean processes and may not yield direct reconstructions of monsoonal precipitation. Oxygen isotopic variations in speleothem and multiple proxies from ocean sediments consistently show that monsoon precipitation increased during the Holocene. The connection between insolation changes and monsoon needs to be carefully reassessed.

Keywords: Corals, Holocene, Indian Ocean, monsoon, oxygen isotopes, speleothems, stable isotopes, tree rings.

Introduction

THE Indian summer monsoon (ISM) exhibits variance over intra-annual, annual, decadal, centennial and millennial to multi-millennial time scales[1]. Annual to decadal scale variations are well documented by meteorological data dating back only to 197 years (i.e. since 1813 CE; all dates mentioned hereafter are in Common Era, unless otherwise stated). These limited data have given crucial insights into the underlying physical mechanisms and helped assessing the impact of recent global climate change[2,3] on ISM. For deciphering low frequency variations (i.e. longer timescales), we take recourse to natural climatic archives such as tree-rings, corals and ice-cores, which provide proxy data of past monsoon variations with a high time resolution (1 year or less), and speleothems and ocean sediments, which do the same, albeit with a coarser resolution (annual to decadal). The process of transforming such proxy data into the relevant climatic parameter (e.g. monsoon rainfall) is usually referred to as 'reconstruction' in the palaeoclimatic literature.

The Arabian Sea offers an excellent opportunity to study past monsoon variability as it experiences intense biogeochemical changes during the monsoons, which get recorded in corals and sediments[1]. Of several studies that tried to reconstruct past ISM, longer records (tens of thousands of years) show that it was stronger during the interglacial and weaker during the glacial periods, whereas the winter or the Northeast monsoon (NEM) exhibited the opposite behaviour. Several forcing factors postulated to explain the monsoon variability on different timescales (decadal to millennial) include both internal (such as oscillations in ocean–atmosphere system, changes in atmospheric concentration of greenhouse gases, volcanism, clouds, ice and vegetation cover) and external causes (insolation changes due to Milankovitch cycles and changes in the solar activity itself). Recent high-resolution studies have revealed that, akin to fluctuations shown during Pleistocene glacial and interglacial stages, monsoon shows a high variance within the present interglacial as well.

The present interglacial period, the Holocene (i.e. the last 11,700 years), though considered to be a period of relatively unvarying warmth, was punctuated by intervals of abrupt changes such as the 8.2 kyr cold event[4]. The Holocene is the only interval in the geological time-scale whose boundary (the Pleistocene–Holocene boundary) is defined climatostratigraphically in contrast to other Phanerozoic epoch boundaries which have been defined biostratigraphically. The base of the Holocene is fixed in the North Greenland Ice Core Project (NGRIP) ice-core record at the horizon showing the clearest signal of climatic warming, an event that marks the end of the last cold episode (Younger Dryas Stadial/Greenland Stadial1) of the Pleistocene[5]. In calendar years, the base of the Holocene would be close to 11,700 yrs BP (Before Present refers to before 1950 CE).

*For correspondence. (e-mail: rramesh@prl.res.in)

Subdivisions of the Holocene

Though no formal subdivisions of the Holocene epoch have yet been proposed by the International Stratigraphic Commission, several authors loosely use the terms 'early Holocene', 'mid Holocene' or 'late Holocene' when referring to climate changes observed during various time intervals in the last 11,700 years. In the absence of any formal division, overlap in the usage might continue; here, we specify the time interval in years and use the terms early, middle, or late Holocene only to maintain the terminology of an earlier reference. One of the earliest subdivisions of the Holocene was proposed by Axel Blytt and Rutger Sernander (the Blytt–Sernander Sequence[6]), based on the pollen stratigraphy of Swedish peat bogs.

Holocene climatic changes can thus be considered as perturbations in the overall warmer period which began ~11,700 yrs BP after the short spell of the cold Younger Dryas interval. The scarce record of Younger Dryas in many parts of the world itself puts constraints on recognizing the Pleistocene–Holocene boundary. This is a problem common to all chronostratigraphic definitions. Whenever a standard Global Boundary Stratotype Section and Point (GSSP) is proposed, it is based on some record of some characteristic facies, which often differs from the one that is being studied and correlated with the type locality. In the case of Holocene, the facies of GSSP is ice. Thus, for marking the base of the Holocene in a locality in India, one is ideally supposed to find the end of Younger Dryas episode (event-wise) or simply get a radiocarbon date close to 10,000 yrs BP (chronometrically). The demarcation of the Holocene for any marine sedimentary or limnic sequence in tropical countries would be based on chronometrically determined level rather than a strong signal of termination of the Younger Dryas.

In this article we summarize the current status of quantitative palaeomonsoon reconstruction from reliably dated palaeoarchives; for the sake of brevity, we limit ourselves to oxygen isotopes and refrain from discussing other proxies, except in the case of tree rings and ocean sediments. We focus on selected tree-ring, coral, ice-core, and speleothem and sea sediment studies, because they have been dated with a high time resolution (e.g. ring counting/accelerator mass spectrometry (AMS) dates) from different regions in India and the Indian Ocean (IO). Figure 1 shows the sample locations.

Tree-rings

The growth of the trees is affected by climatic parameters such as rainfall and temperature[7]. Thus the diametric growth of a tree during the growing season of a year is a function of the intensity of these parameters during that year. Annual growth can be quantified in terms of the ring-width, a proxy for the intensity of the growth-limiting conditions during that year. Stable isotope ratios of oxygen (δ^{18}O), hydrogen (δD) and carbon (δ^{13}C) of tree cellulose also preserve climate signatures of the respective years (see ref. 8 for a recent review). Coherence of the isotopic signal within individual trees and among trees at a given site makes them highly suitable for reconstructing regional past climate[9]. δ^{18}O and δD of tree cellulose depend upon δ^{18}O and δD of precipitation, which in turn depend upon the amount of precipitation in the tropics and ambient temperature in mid to high latitudes. δ^{13}C is known to be affected by temperature, soil moisture and relative humidity; the latter two are often influenced by the amount of precipitation. Thus, the replicated width and isotopic ratios of well-dated tree rings can potentially yield climate data over a few centuries. In peninsular India, the growth-governing parameters are rainfall and soil moisture[10,11], whereas in the Himalaya, they are precipitation and temperature[12–14]. The correlation observed between the amount of rainfall and its isotopic composition, known as the amount effect[15], is known to be reflected in the isotopic composition of tree rings[16].

Ring-width

Only a few trees from peninsular India show datable annual growth rings. Teak (*Tectona grandis*) and toona

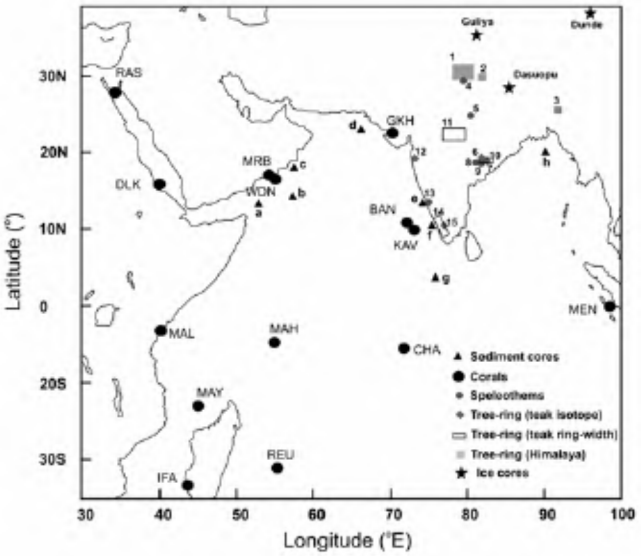

Figure 1. Sample locations of proxy records. Coral (black circles) and ice core (stars) δ^{18}O records downloaded from the website of the World Data Center for Paleoclimatology (http://www.ncdc.noaa.gov/paleo/corals.html). RAS: Rass Umm Sidd[38]; DAL: Dahlak Archipelago[42]; MRB, WDN: Marbat, Wadi Ayn, Oman coast[41]; GKH: Gulf of Kutch[40]; BAN: Bangaram Island[44]; KAV: Kavaratti Island[43]; MEN: Mentawai Island[59]; CHA: Peros Banhos Atoll, Chagos Archipelago[47]; MAH: Mahe Island[46,47]; MAL: Malindi, African coast[48]; MAY: Mayotte; IFA: Ifatey, Madagaskar[56]; REU: La Reunion Island[51]. For sediment cores: 'a' is ref. 110; 'b' is ref. 88; 'c' is ref. 93 and 100; 'd' is ref. 104; 'e' is ref. 85; 'f' is ref. 108; 'g' is ref. 107; 'h' is ref. 126. Other symbols are explained in the legend.

(*Cedrela toona*) are the two prominent examples[17]. The usefulness of ring-width variations of teak trees from central India in the reconstruction of past rainfall has been amply demonstrated[10,11,18,19].

On the basis of analysis of teak trees from central and southern India, a significant correlation of ring-width with pre-monsoon and post-monsoon climate was shown[11,18] and the role of a moisture index rather than total rainfall as the major factor controlling ring-width variations, inferred. 'Moisture index' is a measure of water balance of an area in terms of gains from 'monsoonal rainfall', i.e. precipitation and losses due to evapotranspiration. Ring-width variations of teak from Hoshangabad, Madhya Pradesh were reported to be controlled by monsoon precipitation (June to September)[10]. The rainfall reconstructed (for the period 1835–1997) from ring-width variations of teak trees indicated major droughts over the region[10]. Recently a Monsoon Asia Drought Atlas (MADA) has been created from tree-ring records in Asia, which provides a seasonally resolved gridded spatial pattern of Asian droughts over the past millennium[19]. This could reproduce the East Indian drought (1790, 1792–1796) and the late Victorian Great drought (1876–1878). These data, though represent only a few samples from the Indian subcontinent, could help understand the linkage between monsoonal rainfall and its forcing factors.

A teak ring-width record from Kerala[20] for the past 523 years (1481–2003), the longest till date, revealed the connection between ring-width and El Niño-southern oscillation (ENSO)-related drought, primarily through a distinct association between years of deficient rainfall and poor tree growth. In addition to ring-width variations, early wood vessel size of teak from Parambikulam, Kerala was shown to preserve information regarding rainfall during October to November (NEM) of the previous year[21]. The NEM rainfall reconstructed for the period 1743–1986 showed higher rainfall during 1760–1790.

The Himalayan region offers tree-ring records spanning the last millennium[22–24]. Ring-width variations of trees from moisture stressed sites have been employed for the reconstruction of past precipitation. In general, tree-ring attributes (ring-width and ring-density) are positively correlated with precipitation from October of a year to May of the next year, and hence are potentially useful for the reconstruction of pre-monsoon (March–April–May) precipitation[25,26].

A strong relationship between ring-width indices of *Cedrus deodara* and spring (March to May) precipitation was found in Uttaranchal, western Himalaya[26]. This study revealed the highest (from 1977 to 1986) and lowest (from 1932 to 1941) precipitation events during 1731–1986 (Figure 2 *a*) and an increasing precipitation trend post-1970. This relationship was later seen farther[27] back in time to 1560 (Figure 2 *b*). A similar reconstruction for the period 1310–2004 was developed for Kinnur region, Himachal Pradesh[28]. This, however, did not show an increasing trend of precipitation during the late twentieth century, highlighting significant regional differences. Sensitivity to March precipitation was also observed in *Pinus kesiya* from Shillong Himalaya[29].

Isotopes in tree cellulose

Isotopes in trees have an edge over ring-width based studies as the former are less affected by non-climatic factors[30]. A positive correlation between cellulose δD and local rainfall found in teak trees from western India[30] was recently confirmed by the δ^{18}O record for teak cellulose from western and central India[16]. This positive correlation is contrary to expectation in the tropics; because higher rainfall corresponds to lower δ^{18}O values according to the amount effect. The positive relationship is attributed to the link between the length of the growing season and rainfall. Thus δ^{18}O (and δD) records of Indian teak can be useful even in regions where the amount effect is absent or only weakly present (e.g. Mumbai).

In contrast, teak from southern India showed a negative correlation with local rainfall, implying a relatively stronger amount effect over longer time scales[16]. Using the δ^{18}O of teak cellulose, rainfall of southern India was reconstructed[16] back to 1743 (Figure 3), extending the existing regional and local rainfall records by 70 and 128 yrs respectively. This extended record revealed higher rainfall during the later part of the Little Ice Age (LIA) over southern India.

The potential of cellulose δ^{18}O, δD and δ^{13}C of *Abies pindrow* in reconstructing the past precipitation and

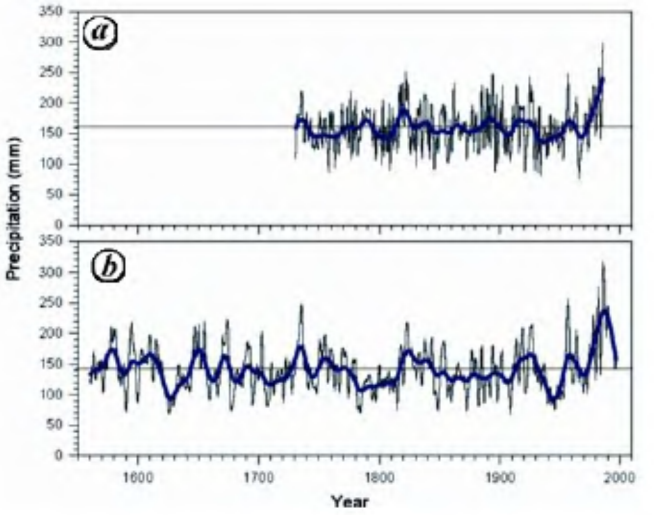

Figure 2. Pre-monsoon (March–April–May) precipitation reconstruction using tree-ring data network of Himalayan cedar from Bhagirathi and Tons basins. ***a***, 1731–1986 reconstruction from a network of 15 ring-width chronologies; ***b***, 1560–1997 reconstruction from a network of longer series from 13 sites in Bhagirathi and Tons basins. The smooth line is a 20-year low pass filter[159].

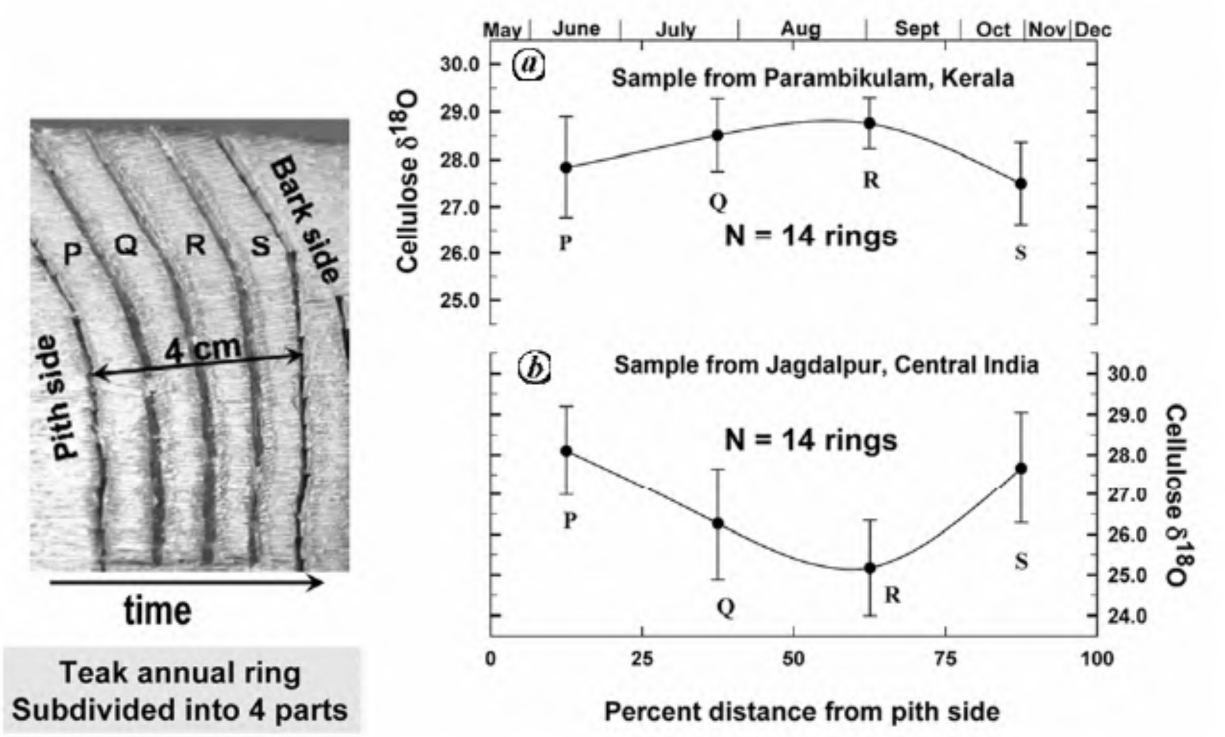

Figure 3. Intra-annual oxygen isotope analysis of teak. The photograph shows scheme of intra-annual sampling. Figure shows intra-annual oxygen isotope variations of teak rings from Parambikulam, Kerala (*a*) and Jagdalpur, central India (*b*).

associated features such as cloud amount and relative humidity was established[31]. The usefulness of a tree-ring $\delta^{18}O$ chronology of *Abies spectabilis* from Nepal for reconstructing past rainfall during monsoon season (June to September) and quantifying temporal variation of ENSO–monsoon relationship was also recently demonstrated[14]. In contrast to ring-width, isotopes clearly showed evidence for LIA in the Himalaya[32].

Intra-annual isotope studies of teak

Taking advantage of a recently developed faster cellulose extraction technique and a plant physiological model developed for interpreting the $\delta^{18}O$ record of tree cellulose, Managave *et al.*[32–34] demonstrated the potential of using intra-annual cellulose $\delta^{18}O$ of teak in reconstructing past climate on seasonal time scales. A clear annual cycle in intra-annual $\delta^{18}O$ variations in teak trees from central and southern India enabled them to identify growth during the pre-, main- and post-monsoon seasons. Hence, it appears possible to establish the chronology of trees lacking discernible growth rings using wood corresponding to one seasonal cycle of $\delta^{18}O$ as a 'ring' and dating/counting to assign calendar years to it.

Break monsoon conditions, viz. an abrupt weakening of rainfall during the rainy season, is an important factor leading to drought. Inter-annual variations in the seasonal pattern of $\delta^{18}O$ of teak cellulose from central India were found to be correlated with relative humidity[32]. So past break-monsoon conditions associated with lower relative humidity could be recognized from high resolution intra-annual sampling of tree growth[32].

Opposite patterns in intra-annual cellulose $\delta^{18}O$ of teak trees were observed in central and southern India[32–34] (Figure 4). Southern Indian teak (from Parambikulam, Kerala) revealed lower values at the ring extremities and higher values at the middle whereas central Indian teak (from Jagdalpur, Chhattisgarh) showed the reverse. Modeling[34] revealed that this can be explained only if the teak from southern India preserved the signatures of both ISM and NEM (more depleted in ^{18}O) during the main and late growing seasons respectively. Thus past years with excess of NEM, associated with the El Niño events, could be identified from the $\delta^{18}O$ of the latewood in southern Indian teak trees.

Scope of future work on tree ring $\delta^{18}O$

A good number of tree-ring chronologies, conifers from the Himalaya and tropical species from peninsular India dating back to 500–1000 years are available for isotope measurements. In the latter, intra-annual isotope measurements could yield high resolution reconstructions of both the summer and winter monsoons, buttressed by oxygen isotope measurements of speleothems from the same localities.

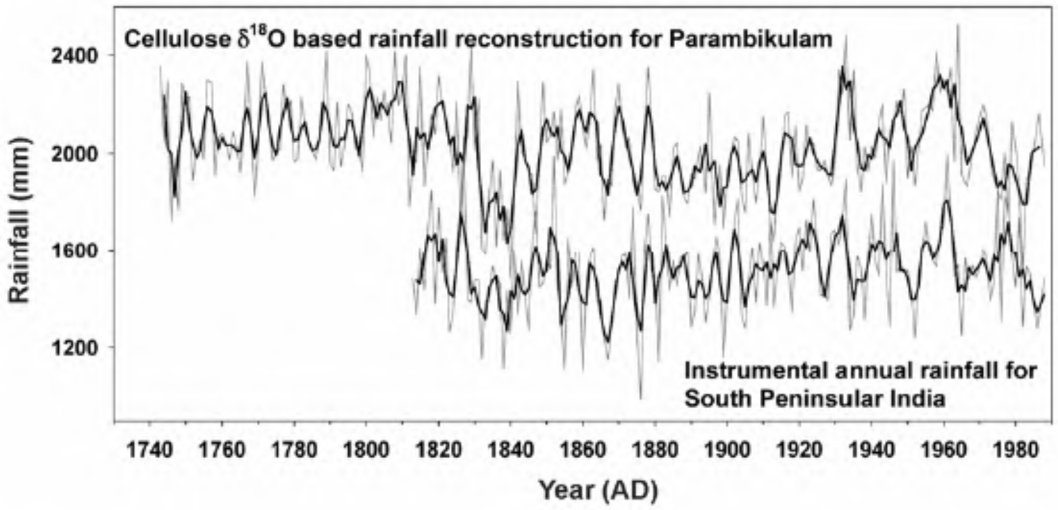

Figure 4. Comparison of instrumental rainfall record for south peninsular India and rainfall reconstructed using oxygen isotope analysis of teak from Parambikulam, Kerala[16].

Corals

δ^{18}O of corals from the IO has proven useful in understanding interannual and decadal scale variabilities of ocean atmospheric processes. δ^{18}O of reef building corals is a function of sea surface temperature (SST) and δ^{18}O of the ambient sea water. A well constrained relationship between SST and coral δ^{18}O can reveal the dynamics of the SST variability as controlled by ocean atmospheric processes. IO climate, including the intensity of the Asian monsoon variability, shows some degree of correlation with ENSO[35]. The Pacific ENSO greatly affects SST and precipitation in IO. δ^{18}O of corals growing in IO has given insights into the interaction between ENSO and climate. Some such records are shown in Figure 5.

Northern Arabian Sea

A number of coral records have been obtained from the northern Arabian Sea including the Red Sea. A 245-year coral δ^{18}O record from the northern Red Sea[36] (Ras Umm Sidd in Egypt; 28°N, 35°E) shows a strong coherence at a period of 5.7 yr (*op. cit.*) with ISM rainfall (ISMR). This led to the hypothesis that the Asian monsoon controls the eastern Saharan and the eastern Mediterranean subsidence and aridity.

Analysis of instrumental data and modelling confirms that the Arabian SST influences the subsequent monsoon rainfall on timescales of less than a month. A low Arabian SST leads to a reduced Indian rainfall and vice versa[37–39]. The oxygen isotope record of a *Favia* coral collected from the Gulf of Kutch (22°6′N, 69°30′E) indeed showed such a relation with the monsoon rainfall[40]. The δ^{18}O (i.e. SST maxima) of coral from the Gulf of Kutch and the total monsoon rainfall in the Kutch and

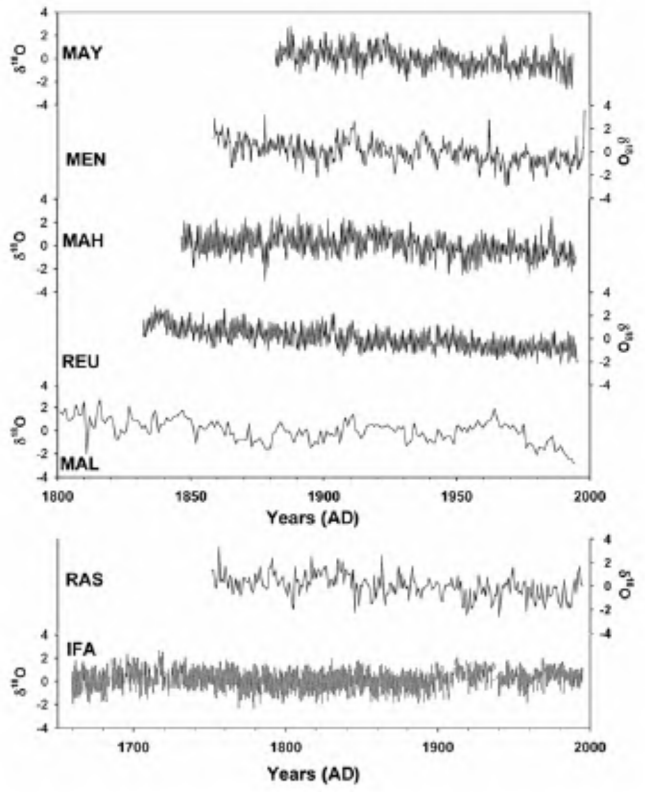

Figure 5. δ^{18}O records of various corals from the Indian Ocean. The *y*-axes represent the normalized variations of δ^{18}O of the respective corals. Only those records have been plotted whose data sets were available in the website of the World Data Centre for Paleoclimatology. Locations are shown in Figure 1.

Saurashtra region (1949–1989) were inversely correlated (linear correlation coefficient $r = -0.56$, significant at $P = 0.01$ level). As coral oxygen isotope ratios are inversely related to SST, a lower coral oxygen isotope ratio would imply higher SST and lower rainfall, as supported

by observations[40]. The Gulf of Kutch coral, however, does not show any significant correlation with ISMR.

In contrast, a significant inverse correlation ($r = -0.50$, $P = 0.05$) between ISMR and $\delta^{18}O$ in a *Porites* coral collected from Marbat, Oman coast (16°50′N; 54°45′E) has been reported[41]. The correlation improved to $P = 0.01$ when the linear trend of the $\delta^{18}O$ time series was removed. Surprisingly $\delta^{18}O$ of another coral collected from a nearby location, Wadi Ayn (16°48′N; 54°50′E) failed to show a significant relationship with ISMR, as also a combination of the two data sets. But when the combined time series was detrended, a significant relation with the annual rainfall was evident ($r = -0.5$, $P = 0.05$).

Periodicities of 5 and 2–2.5 yrs were found in the $\delta^{18}O$ record of a coral from the Dahlak Archipelago[42] (15°43′N, 39°54′E). It was weakly coherent with the Indian Ocean SST, and Southern Oscillation Index (SOI). The weak coherence implies that the coral $\delta^{18}O$ record is not linearly related to either the Indian Ocean SST or SOI at these periods. However the presence of spectral peaks does suggest the influence of ENSO style dynamics on coral $\delta^{18}O$.

Central Arabian Sea

There are many coral islands in the Lakshadweep Archipelago. Two short coral $\delta^{18}O$ records from Kavaratti (10°N, 73°E) and Bangaram islands (10°55′N; 72°17′E) have been reported[43,44], the latter affirming the findings of the former. Coral $\delta^{18}O$ from this region is by and large controlled by SST and modulated by wind-induced vertical mixing and hence can facilitate reconstruction of SST variability[45] in the past. A spectral analysis of the $\delta^{18}O$ record of the Bangaram coral shows a periodicity of 5.2 yr (90% significance level), which is attributed to the ENSO forcing[44]. Interestingly, neither of these corals shows a correlation with local precipitation or ISMR.

Western Indian Ocean

The western IO, notably the equatorial region of the IO, is strongly influenced by ENSO as inferred from several coral records, such as the ones from Mahe[46,47] (4°37′S; 55°49′E), Seychelles and Malindi in the Kenyan coast[48] (3°S; 40°E). A 3-m long coral (*Porites lutea*) from Mahe was used to reconstruct a 150-year record of the equatorial IO climate variability and to distinguish between interannual ENSO-related variability and decadal variability believed to be associated with the Asian monsoon[46]. Periodicities of 5–6 yr and 10–12 yr were found to be coherent with Niño 3.4 SST. The 5–6 yr periodicity has been linked to the ENSO variability, but the coupling of the 10–12 yr periodicity to the ISMR is questionable. Cole *et al.*[48] analysed both the Seychelles and the Malindi $\delta^{18}O$ records and concluded their decadal variance was more coherent with ENSO indices and neither of the two corals showed any significant representation of ISMR or east African rain. They observed that the two coral records were coherent with each other at the above periodicities. This suggests that the IO decadal variability reflects decadal ENSO-like variability originating in the Pacific but not monsoon forcing.

Another coral sample[47] (North East Point, NEP) from Seychelles gave a continuous coral $\delta^{18}O$ record for the period 1840–1994. A composite coral $\delta^{18}O$ time series based on a simple arithmetic mean of the time series of NEP coral and the Seychelles coral[46] was better correlated with SST and other climatological parameters than the individual time series.

Cross-spectral analysis of the MAHE record (November–February) and Niño 3.4 index revealed three distinct peaks in the coherency spectrum, centred at 16–10, 5.8–4.7 and 3.5 years; the latter two peaks were attributed[47] to ENSO, which illustrates the strong coupling between the tropical Pacific and Indian Oceans on interannual time scales. The analysis also confirms that the decadal climate variability in IO is influenced by the tropical Pacific[48]. The effect of Pacific decadal forcing and absence of monsoon forcing and the strong influence of the SE trade winds on the MAHE coral implied[47] that the corals from the western equatorial IO primarily record SST changes in response to the strength of the SE trade winds, which are an integral component of the Asian monsoon system[49,50]. An implication of this observation is that the amount of rainfall over India is not necessarily related to the intensity of the SE trade winds, which determine the summer cooling in the Arabian Sea[50]. However the coral records do not provide any clue to the *origin* of decadal-scale ENSO-like variability in IO.

Central Indian Ocean

Two *Porites* sp. corals[51,52] from the Chagos Archipelago (7°S, 72°E) in the geographical centre of the IO, have yielded a 120-year long (1870 to 1990 AD) $\delta^{18}O$ time series that clearly show the temporal variations in precipitation associated with the Inter Tropical Convergence Zone (ITCZ). The inter-decadal oscillations in coral $\delta^{18}O$ appear to record not the regional SST changes but the $\delta^{18}O$ of seawater modulated by the ITCZ precipitation during the NE monsoon. This is consistent with the observation that SST and Outgoing Longwave Radiation (OLR) are weakly correlated in IO[49].

The most significant feature of this coral record is the shift from interdecadal to interannual variability in the late 1970s, which is not known in its earlier history. This shift is most pronounced in the rainy season and, hence, interpreted[51] as a change in precipitation pattern associated with ITCZ. It was proposed[52] that the IO SST warming contributed to the observed climate shift over the

central equatorial IO sector by a nonlinear linkage between SST and deep convection.

The inter-decadal oscillations in coral $\delta^{18}O$, if driven by ITCZ precipitation, imply that (i) the SST in the tropical IO is not regulated by deep atmospheric convection, as has been proposed for the tropical Pacific[53,54], and (ii) atmospheric convection is governed by processes other than ocean–atmosphere interactions[49]. It was suggested[49] that in the IO, deep convection is determined by dynamic atmospheric processes or instabilities. The Chagos coral record indicates that even on decadal to centennial time scales, atmospheric convection is not related to regional SST variations in the central IO. Therefore, interdecadal variations of ITCZ should be due to other processes, possibly atmospheric dynamics[51].

South Central Indian Ocean

Several coral oxygen isotope records from the subtropical and tropical areas of the south central IO, including samples from the tropical IO (Ifaty reef; 23°S, 43°E) off Madagascar, La Reunion Islands (21°S, 55°E) and Mayotte (13°S, 45°E) were studied[53–57]. The Mayotte and Ifaty corals recorded changes in the hydrological balance, whereas the Reunion coral recorded multi-decadal variations in salinity propagated via changes in the strength of the South Equatorial Current. All these records showed non-stationary behaviour in ENSO-proxy relationships and/or higher sensitivity to ENSO induced large-scale circulation anomalies when the forcing was strong. However the NEP coral record from Seychelles studied by the same group[47] showed a stationary relationship with ENSO.

Eastern Indian Ocean

Analysis of coral oxygen isotope from the eastern IO has attracted much attention recently, as it can be related to the present and past behaviour of the Indian Ocean Dipole (IOD), an interannual climate mode of variability in the IO[58]. Instrumental records of IOD, i.e. the IOD index are available only for the last fifty years. Abram *et al.*[60] analysed coral samples from the Mentawai Island arc, located approximately 200 km off the Sumatra coast in western Indonesia. A zonal gradient of coral $\delta^{18}O$ was calculated from the eastern[59,60] and western[46,47] coral records. The IOD index since 1846 was reconstructed and an increase in the frequency and strength of IOD events during the twentieth century was observed, associated with enhanced seasonal upwelling in the eastern IO. They further predicted[60] that projected greenhouse warming may lead to a redistribution of rainfall across IO and a growing interdependence between IOD and Asian monsoon precipitation variability. Reconstruction of surface-ocean cooling and drought during individual IOD events over the past 6500 years using another fossil coral (Mentawai) was attempted[61]: IOD events during the middle Holocene were characterized by longer durations of strong cooling of the ocean surface, together with droughts that peaked later than those expected by El Niño forcing alone. A suite of living corals from the Indian and Pacific Ocean indicated a strong zonal oxygen isotopic gradient in IO, which was significantly correlated with central Pacific SST on a variety of timescales. It was interpreted as due to a strong ENSO-like teleconnections over IO and not specific to IO or monsoon dynamics[61].

Scope of future work on coral $\delta^{18}O$

The $\delta^{18}O$ corals in IO are influenced by different ocean atmospheric processes. The coral $\delta^{18}O$ from the northernmost region (i.e. Northern Red Sea) appears to be controlled mostly by the North Atlantic Oscillations, whereas that from southern corals, on decadal time scale shows a strong dependence on the winter surface water influx to the Red Sea from IO, modulated by IO SST. The corals off Oman show a significant correlation with the NEM rainfall, but only a weak correlation with ISMR. Corals from the NE Arabian Sea depend mostly on local ocean–atmospheric processes, whereas corals from the central Arabian Sea depend largely on SST, and register the surface cooling due to upwelling. The effect of ENSO on coral $\delta^{18}O$ in this region remains unclear.

The West IO displays a strong teleconnection with the Pacific ENSO and hence the corals in this region strongly respond to the ENSO activity. This has helped in relating the IO decadal variability to the decadal ENSO-like variability originating in the Pacific but *not* to the monsoon forcing. The central equatorial IO corals are sensitive to the sea water $\delta^{18}O$ that is greatly affected by the seasonal precipitation during the boreal winter, whereas the corals farther south are affected by the SE trade winds and the hydrological balance of the region; so these corals might be useful in reconstructing past rainfall associated with the movement of ITCZ. The correlations with ISMR, however, are neither strong nor consistent enough to permit its reconstruction from coral $\delta^{18}O$-rainfall relationship. The great challenge that lies ahead is to reconstruct the ISMR with sub-annual to annual resolution from coral proxies.

Ice cores

Oxygen isotopic variations in ice-cores from the Himalaya and Tibet (Figure 1) are shown in Figure 6. These records from the Dundee, Dasuopu and Gluiya ice caps[62–67] show a warming trend since 1800, but different trends earlier. The mean $\delta^{18}O$ values also are quite different from what is expected: Guliya and Dundee, which lie father north, show mean values of −14‰ and −11‰ respectively,

whereas the ice core closest to monsoon region shows a mean value of –20‰. At least three competing processes need to be disentangled before a meaningful or unequivocal interpretation can be made of the oxygen isotopic variations. These are the amount effect, seasonality of precipitation and temperature. In addition, atmospheric dynamics could also play a role[67].

Scope of future work on ice-core $\delta^{18}O$

Oxygen isotopes from more ice cores, with a proper calibration of isotopes in precipitation with ambient climatic parameters, could clarify whether the monsoon rainfall could be reconstructed. Choice of a sensitive glacier in the Indian side of the Himalaya, where summer melting and re-freezing does not alter the isotopic signatures is crucial for the success of this endeavour.

Speleothems

Caves are amongst the longest-lived features of landscapes surviving for millions of years. The most preferred archive for palaeoclimatic reconstruction after tree-rings and corals are speleothems. Speleothems refers collectively to all types of minerals (stalagmites, stalactites and flowstones) growing in natural caverns. Stalagmite, a column-shaped speleothem forming on the cave floor, is like an inorganic tree growing for many thousands of years. The cover of overlying bedrock and soils protects them against erosion and weathering. Calcitic stalagmites, stalactites and flowstones are useful for the environmental reconstruction. Aragonite and gypsum speleothems have received less attention because of their rare occurrence and structural instability[68]. Speleothems have been dated by radiocarbon (^{14}C) and U–Th methods. Samples have to be carefully selected to avoid spurious radiocarbon and U–Th dates. For example, varying fraction of dead carbon derived from bedrock in a speleothem may result in spuriously older radiocarbon dates[69,70]. ^{14}C method cannot date samples older than 50 ka. High concentration of fine dust (detrital) can lead to many ionic species in seepage water to invalidate U–Th ages[71]. Speleothems from caves in five different climatic zones in the country have so far been analysed for generating a land-based ISMR record.

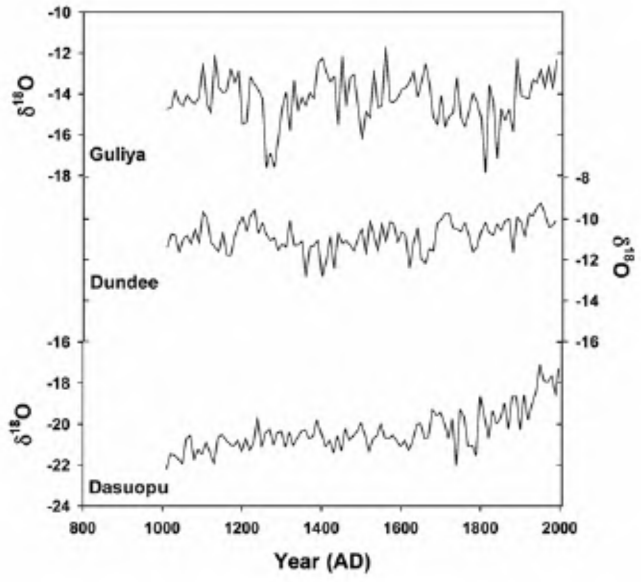

Figure 6. $\delta^{18}O$ of ice cores from the Himalayan-Tibetan region.

Dandak cave, Jagdalpur district, Chhattisgarh

This cave has two chambers[72] with the first chamber (chamber-1) accessible through a narrow entrance and connected to the second chamber (chamber-2) through a narrow passage. ISMR was reconstructed[69,70] initially for two time periods, 0–1200 yr and ~3200–3700 yr based on radiocarbon dates of stalagmite collected from chamber-2. Using U–Th dating chronology was extended to 0–1.6 ka and 2.8–5.6 ka. Another fossil stalagmite from chamber-2 was dated to have grown during 9.1–10.4 ka (ref. 73). $\delta^{18}O$ records of these two stalagmites from chamber-2 indicate that ISMR was lower during the early Holocene (Figure 7) and gradually increased to the present[73]. Trace levels of Sr, Mg and Ba found in speleothems reflect rainfall variation, and Mg also as a proxy of past temperature variations[74]. High-resolution monsoon reconstruction from a stalagmite collected from chamber-1 and U–Th dated between 400 and 1300 yr BP reveals ISMR variations[75] such as severe droughts lasting several decades in the fourteenth and mid-fifteenth centuries. Several distinct charcoal beds in chamber-2 dating between ~4 ka and 7 ka point to human habitation in the Dandak cave in the past[72].

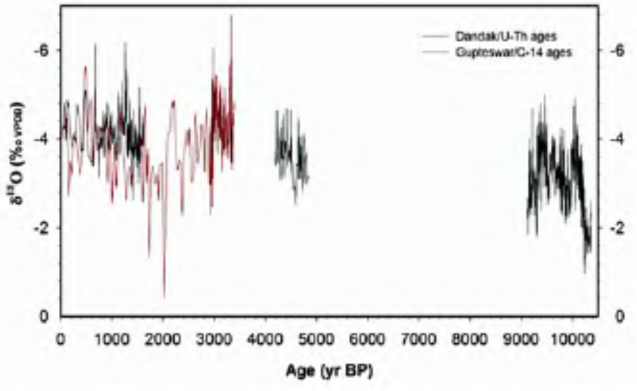

Figure 7. Temporal variations in the $\delta^{18}O$ of the Dandak stalagmites (black line) and Gupteswar stalactite (red line). Depleted and enriched $\delta^{18}O$ suggests respectively enhanced and reduced monsoonal conditions. Dandak record was generated using two stalagmites from chamber-2.

Akalagavi cave, Uttar Kannada district, Karnataka

Akalagavi is a small cave located near coastline of a peninsular tropical dense forest[76]. An actively growing stalagmite collected from this cave showed annual laminations spanning 331 years from 1997 to 1666. In the period covered by instrumental record, depleted and enriched $\delta^{18}O$ spikes in the stalagmite are correlatable with flood and drought years seen in the rainfall record, within a few years of uncertainty[76]. Moreover, during several drought events shown by the instrumental record between 1850 and 1920, a clustering of wavelet power associated with 21-year sunspot cycle is detectable in the $\delta^{18}O$ data[77]. Such correlations clearly show that speleothem $\delta^{18}O$ responds to ISMR variations.

Gupteswar cave, Koraput district, Orissa

A monsoon record of the past ~3000 yr has been constructed from an actively growing stalactite collected from this cave and dated by radiocarbon method[69,70]. A combined plot of $\delta^{18}O$ in Dandak stalagmites and Gupteswar stalactite is presented in Figure 7. This shows that monsoon varied significantly during the Holocene, with a significantly lower rainfall around 2000 yr BP and higher rainfall at ~ 3200 yr BP.

Sota cave, Chitrakoot district, Uttar Pradesh

A stalactite from a narrow chamber of this cave[78] has provided rainfall data for the past ~2800 yr. This record shows similarities and differences as compared with the Dandak and Gupteswar reconstructions. They were attributed to regional and local climatic changes[79].

Timta cave, Pithoragarh district, western Himalaya

A stalagmite dated by the U–Th method recorded varying ISMR between 11.5 and 15.5 ka (ref. 80).

These reconstructions demonstrated that speleothem $\delta^{18}O$ reflects the 'amount effect' – a negative correlation between $\delta^{18}O$ of monsoon precipitation and amount of precipitation. Such an effect arises from convective condensation during which ^{18}O enriched molecules are preferentially removed leaving the $\delta^{18}O$ of the remaining vapour increasingly lighter. A strong convective process results in higher amounts of precipitation; and hence the isotopic composition of rainwater is depleted[81,82].

It is now recognized that only certain caves and speleothem are suitable for palaeoclimatic research, as $\delta^{18}O$ in speleothems can represent extant climatic conditions only if formed near isotopic equilibrium with ambient water. As mentioned earlier, any detrital material inherited by speleothems during growth can lead to spurious age estimates. Also, natural growth of speleothems can be affected by substantial human activities in the vicinity.

Scope of future work on speleothem $\delta^{18}O$

Some more caves are currently under study, such as the Baratang cave in Andaman Islands and Belum caves in Kurnool, Andhra Pradesh[71]. As the isotopic sensitivity of any speleothem to the ambient climate depends upon several factors but primarily on the cave location and the local meteorology, systematic observations of isotopic signatures in modern rain[70,81] and cave seepage water are called for.

Ocean sediments

Sediments in the seas around Indian subcontinent act as an excellent recorder of past monsoon variability[83]. During the ISM season, flow of strong winds parallel to the Somalian and Oman coast causes Ekman divergence and induces intense upwelling in the western Arabian Sea with upwelling velocities close to 3×10^{-3} cm/s and an upwelling transport of 1.5–2 Sv in the upper 50 m (ref. 84). The upwelling of nutrient-rich water in the euphotic zone enhances the productivity considerably and increases the abundance of selected foraminiferal species (such as *G. bulloides*), the signature of which gets preserved in the underlying sediments and thus record the signatures of ISM winds. On the other hand, copious orographic precipitation over the Western Ghats during ISM reduces the sea surface salinity considerably along the southwestern coast of India in the Eastern Arabian Sea[85]. This influx of freshwater reduces the $\delta^{18}O$ of seawater; the $\delta^{18}O$ of calcareous tests of foraminifera registers these changes and hence reflects ISM precipitation. During ISM, coastal southwest India also experiences weak upwelling[86,87]. In northern Bay of Bengal, during the summer monsoon season there is a huge influx of fresh, low salinity waters via the Ganges–Brahmaputra River system; the peak summer discharge is 50,000 m^3/s that reduces the mean salinity and the sea surface $\delta^{18}O$ that gets stored in planktic foraminifera. We present here few selected studies chosen because of their highly resolved, well dated nature (accurate AMS dates) from different regions of the Arabian Sea and Bay of Bengal that helps to decipher monsoon variability in different timescales, viz. multi-millennial (sub-Milankovitch) to sub-centennial during the Holocene. For a more exhaustive compilation of studies from the seas around India, readers may refer to Tiwari *et al.*[1].

Sub-Milankovitch timescale (long-term) variability

In one of the earliest high-resolution studies[88], Dolomite content in the core 74 KL off the Oman margin was found to reflect aridity, as when the SW monsoon winds were weak, the dolomite content increased as the northwester-

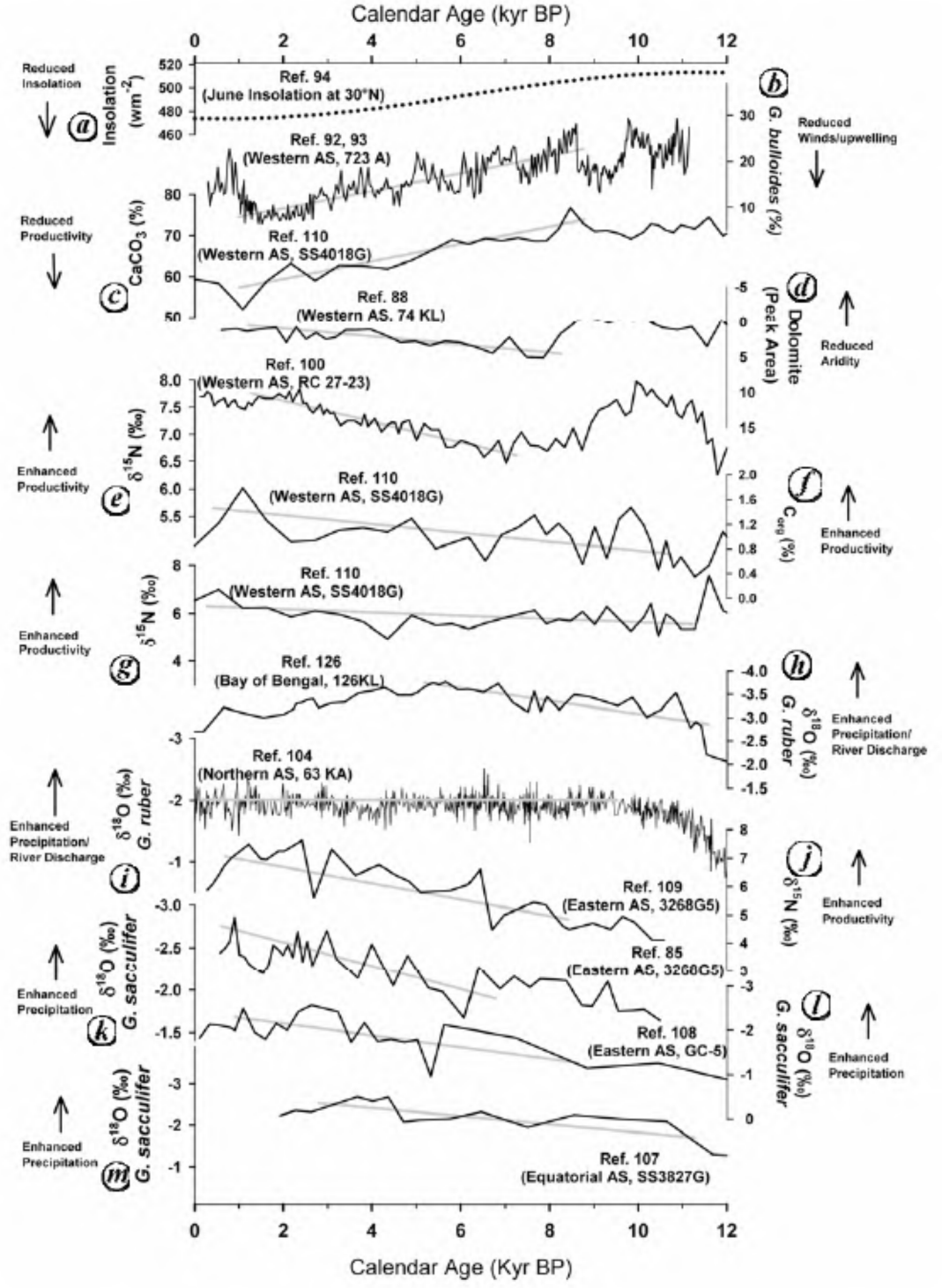

Figure 8. Monsoon variability from different locations/proxies; the pelagic carbonate production declined (***b*** and ***c***) in contrast to other productivity/precipitation proxies; the grey lines represent the visually determined long-term trends; AS: Arabian Sea. Locations are shown in Figure 1.

lies carrying dolomite from the Arabian Peninsula could reach the core site. This dolomite record showed higher monsoonal intensity during the early Holocene followed by a decline at ~8 kyr BP, after which it increased slightly (Figure 8 *d*). It was proposed that the monsoon increased in abrupt step-wise fashion[88]. This inference was confirmed[89] soon based on study of multiple proxies, such as oxygen isotopes, abundance of *G. bulloides* (percentage of *G. bulloides*) and monsoon pollen index in three sediment cores (RC27-24, 23, 28) from the Oman coast. Based on the percentage of *G. bulloides*, pollen index, and a comparison with data from African and Indian

lakes, it was inferred that ISMR peaked during early Holocene (11–5.5 kyr BP) and declined thereafter, lagging behind the peak June insolation by 3 kyr (ref. 89). The percentage of *G. bulloides* fluctuated between 45% (peak monsoon) and 30% (weak monsoon) during the Holocene. It was noted that monsoon pollen index was a more reliable proxy for monsoon maximum because percentage of *G. bulloides* has been reported[90] to saturate above 35–40%. The relative abundance and flux of *G. bulloides* along with total flux of planktic foraminiferal tests from the ODP site 723 A showed[91] that the SW monsoon was relatively stronger between 10 and 5 kyr BP (*G. bulloides* ~45%), after which it declined with the weakest phase at 3.5 ka BP (*G. bulloides* ~35–30%). More recent determination of the abundance of *G. bulloides* from the same site found excellent correlation with the North Atlantic sediment records on centennial timescales (weak summer monsoon coincides with cold periods)[92,93]. It was proposed that monsoon broadly follows the insolation (Figure 8 *a*)[94] with a maximum during early Holocene (11–8.5 kyr BP) and declining since then to ~1.5 kyr BP (Figure 8 *b*)[92,93]. Interestingly, they observed a maximum % *G. bulloides* of ~28% and a minimum of ~10%, which are very different from earlier reports[91] despite the samples being from the same site! Some errors in the earlier papers have been found recently[95]. This coupled with observation that percentage of *G. bulloides* saturates[90] beyond 35–40, cautions us to the risk of relying on a single proxy and stresses the need for multi-proxy analysis.

A perennial oxygen minimum zone (OMZ) between 250 and 1250 m water depths, related to denitrification[96] in the Arabian Sea, occurs due to the high oxygen consumption below the thermocline for the oxidation of organic matter supplied by the high overhead surface productivity driven by monsoon winds[97,98]. The intensity of OMZ and the ensuing denitrification gets recorded in the nitrogen isotopic composition (δ^{15}N) of the organic matter that can be correlated with the overhead productivity intensity and hence to monsoon strength[99]. δ^{15}N (denitrification indicator) and other productivity indicators such as total chlorins and percentage of nitrogen in the core[100] from the Oman margin (RC27-23) spanning the past 60 kyr showed that they are similar. Enhanced denitrification during the early Holocene (11–9 kyr BP) was observed[100], followed by a sharp decline but thereafter it showed a slight increasing trend throughout the Holocene (Figure 8 *e*). This differs significantly from results discussed above[89–91], which show decline in SW monsoon intensity either after mid-Holocene (~5.5 ka) or early Holocene (~8.5 ka)[92,93].

Recently several attempts have been made to retrieve SST in the Arabian Sea, especially the western Arabian Sea[101], which undergoes widespread cooling due to upwelling driven by the SW monsoon wind strength. Using an artificial neural networks technique based on quantitative analyses of planktic foraminifera to construct the annual, summer and winter SST for the last 22 kyr from the ODP site 723 A (ref. 102), it was found out that SST in the western Arabian Sea showed a cooling trend from ~8 ka to the present. This cooling could be an indicator of strengthening upwelling, and hence strengthening monsoon during the Holocene. Another SST reconstruction[103] using two species (*G. ruber* and *G. bulloides*) and percentage of *G. bulloides* from the Somalian margin (western Arabian Sea) focused on glacial–interglacial changes. But a close examination of their Holocene data reveals significant facts – SST stays more or less uniform (based on *G. ruber*) or shows several wide fluctuations but overall a slightly declining trend (based on *G. bulloides*) indicating either unvarying or slightly strengthening upwelling. Interestingly, their percentage of *G. bulloides* record shows an increasing trend from 10 to 4 ka (in contrast to reports from Oman margin[89,91–93]), a decline at 3.5 ka, and an increase thereafter, indicating strengthening upwelling and SW monsoon during the Holocene.

δ^{18}O of planktic foraminifera from the Pakistan margin near the mouth of Indus, which as a proxy of Indus discharge, relatable to the SW monsoon precipitation, indicates that monsoon maintained a more or less uniform intensity[104] during the Holocene (Figure 8 *i*). Similarly there have been a few studies from the equatorial IO[105–107]. One of the studies[107] has shown that δ^{18}O in planktic foraminifera declined in response to declining evaporation–precipitation (E–P), indicating long-term increase in monsoon during the Holocene (Figure 8 *m*).

We now turn our attention to studies from the eastern Arabian Sea that bear on the intensity of ISMR in contrast to the foregoing studies on the record of ISM *winds*.

Very few studies from the eastern Arabian Sea cover the whole Holocene and these multi-proxy studies too do not support a declining monsoon during the Holocene[85,86,103,108,109]. The records off Goa indicate an early Holocene monsoon maxima followed by a sharp decline and then strengthening monsoon till mid-Holocene and a decline thereafter[103]. On the other hand, δ^{18}O of planktic foraminifera in cores further southward off the west coast of India show an overall increase in the SW monsoon precipitation[85,108] but modulated by several millennial scale fluctuations during the Holocene (Figure 8 *k* and *l*). δ^{15}N in cores from the eastern Arabian Sea[109], relatable to changes in surface productivity as inferred from strengthening of upwelling/SW monsoon winds, also reveals several millennial scale fluctuations superposed on the overall trend of increasing denitrification from ~10 to 2 ka, implying increasing SW monsoon during the Holocene (Figure 8 *j*). A recent reconstruction spanning the past ~70 kyr, of ISM from the eastern Arabian Sea[86] also shows an overall decrease in δ^{18}O and hence a strengthening monsoon during the Holocene.

The influx of nutrient-rich waters during upwelling induced by the SW monsoon winds drastically enhances biological productivity in the surface[87], which can be of

several types including organic, carbonate, siliceous, etc. and gets preserved in sediments as relative abundances of organic matter (comprising body-mass of microorganism), calcium carbonate (shells of foraminifera, coccolithophores, pteropods) and silica (shells of diatoms, radiolarians, etc.). To reconcile the apparently contrasting results from the eastern and the western Arabian Sea, a multi-proxy study[110] was conducted in a core (SS4018G) from the western Arabian Sea. Percentages and burial fluxes of $CaCO_3$ (carbonate productivity) and C_{org} (organic productivity) along with isotopic proxies $\delta^{15}N$ (denitrification governed by respiration of organic material) and $\delta^{13}C$ (interplay of productivity, upwelling and seawater carbonate chemistry) were measured[110]. Although the carbonate productivity (percentage and burial flux of $CaCO_3$) shows a decline (Figure 8 *c*) since early Holocene (like percentage of *G. bulloides*), the organic productivity (percentage and burial flux of C_{org}, $\delta^{13}C$, $\delta^{15}N$) stays uniform or shows a slightly increasing trend (Figure 8 *f* and *g*). If the organic productivity did not decline during Holocene, then the question arises as to what diminished the pelagic carbonate production (reducing $CaCO_3$ content and percentage of *G. bulloides*, Figure 8 *b* and *c*).

In the western Arabian Sea, nitrate and phosphate that support calcite productivity show maximum concentrations at ~100 m water depth and decrease below. In contrast, silicate concentration peaks at approx. 175–200 m and even increases downward[111–113]. During the early stages of the SW monsoon, the upwelling commences from shallower depths bringing initially nitrate into the euphotic zone to support pelagic carbonate production/calcitic productivity. As the monsoon progresses, upwelling takes place from deeper layers enriched in silicate[113–115] (200–300 m). This adds sufficient silicate into the photic zone causing diatom blooms[116]. Satellite observations show that diatom blooms cover the whole northwestern Arabian Sea during the later stages of the SW monsoon[114,116]. Thus increased wind strength likely enhances siliceous productivity at the cost of calcareous productivity. This phenomenon (higher silicate productivity and reduced calcareous productivity) has been reported earlier from other regions of the Arabian Sea/IO: (i) higher $\delta^{13}C$ of *G. menardii* (enhanced productivity) and lower $CaCO_3$ content (reduced calcareous productivity)[117]; (ii) higher opal content during the interglacial[118], indicating increased productivity due to upwelling, which would result in higher CO_2 (via organic matter degradation) supply to the bottom waters promoting enhanced dissolution of $CaCO_3$; (iii) pelagic carbonate production decreased[97] in the northern Arabian Sea and was replaced by organic walled and siliceous organisms during times of enhanced productivity as evidenced by C_{org}. Thus biogenic calcareous productivity declines due to increasing SW monsoon wind and is compensated by enhanced biogenic siliceous productivity. This would explain the decline observed in pelagic carbonate production (such as percentage of *G. bulloides* and calcium carbonate content) despite increasing monsoon. Thus during the Holocene SW monsoon did not decline on sub-Milankovitch timescales and in fact showed a slight increase despite a monotonically declining insolation. Internal feedback mechanisms appear to play a dominant role in governing monsoon dynamics on longer timescales, as also corroborated by evidence of monsoon lagging (behind) insolation by several thousand years[119–121].

A few studies of cores from key locations in the Bay of Bengal have also provided long-term records of SW monsoon precipitation based on the huge influx of fresh, ^{18}O depleted water through the Ganges–Brahmaputra–Irrawaddy river system. These studies reported $\delta^{18}O$ of foraminifera[122–125], estimated salinity[126,127], $\delta^{18}O$ of seawater[128] and SST using alkenones or Mg/Ca as proxies. The trends observed from the Bay of Bengal records show an early-Holocene monsoon maximum followed by a decline after mid-Holocene (Figure 8 *h*) unlike the steady decline in insolation[126].

Variability on millennial to centennial and sub-centennial scale

Several studies on strategically sampled, rapidly accumulating sediments and varved sediments have yielded records of ISMR with even sub-centennial time resolution[129]. In one such study involving $\delta^{18}O$ of two different species of foraminifera in a core from the eastern Arabian Sea[130], a prominent arid event is observed at 2 ka followed by other centennial scale dry events centred at ~1.5 ka, ~1.1 ka, ~0.85 ka and ~0.5 ka. These arid episodes are also seen in other proxy records such as reduced thickness and low Ti/Al ratios of varved sediments[131,132], higher $\delta^{18}O$ values of foraminifera in sediment core from northern Arabian Sea[104], and other isotopic and geochemical proxies from eastern Arabian Sea sediments[132]. Comparison with total solar irradiance (TSI) variability shows a clear correspondence between the SW monsoon variability as intervals of lower TSI match those of lower ISMR on centennial timescales[93,133–137]. We noted earlier that monsoon did not follow insolation on longer, sub-Milankovitch timescales but is more influenced by internal feedback mechanisms. But on a centennial scale, ISM monsoon is strongly coherent and hence governed by insolation.

Scope of future work on ocean sediments

Careful selection of fast sedimenting sites in the IO for raising cores, AMS dating of monospecific foraminifera, high resolution oxygen isotopic analyses of different species of foraminifera and multi-proxy studies would widen the data base and enable us to address questions on the

spatial variability of ocean response to various forcings on different time scales.

Spectral analyses and modelling results

Spectral analyses of various summer monsoon proxies indicate that on Milankovitch timescale, ISM is mainly governed by the insolation variations induced by the precessional cycle of the earth's orbit[138,139]. On sub-Milankovitch, multi-millennial timescales, the dominant periodicity exhibited by the monsoon at 1400 ± 500 years[85,126,140] points towards a common forcing factor for ISM and high latitude climatic changes revealing thereby common link between them. On centennial timescales the solar forcing seems to control the ISM variations as evidenced by the common periodicities found in them[93,135,136]. During the Holocene, the solar periodicities dominate whereas those related to Bond cycle (~1500 yr) have been reported to weaken. A synthesis of several studies spanning the past several hundred thousands of years[141] indicates that monsoon exhibits periodicities from tectonic to annual timescales. It comprises cycles such as Milankovitch and sub-Milankovitch (413 kyr, 95 and 124 kyr, 66 kyr, 41 kyr, 30 kyr, 19–24 kyr, 11.5 kyr), bond cycle (1470 yr), solar (900 yr, 700 yr, 510–560 yr, 210 yr, 84–102 yr, 60 yr, 22–24 yr, 11 yr) and ENSO (3–8 yr). This indicates the complex interplay of several forcing factors in modulating monsoon on different timescales. One way to understand the relative contributions of different forcings is via phase lag analysis. Initial studies indicated varying degree of phase lags between the summer-monsoon maxima and the northern hemisphere (NH) summer insolation maxima and ice-volume minima in the precession frequency band. In the obliquity band, the summer-monsoon maxima are in phase with the NH summer insolation maxima while they lead the ice-volume minima, indicating that simple glacial–interglacial forcings cannot explain the monsoon variance and an additional factor namely the latent heat export from the southern subtropical IO[142] needs to be considered. Other studies have attributed the observed lag to increased insolation at the end of summer[98], a more direct influence of insolation and ice-volume[90], or a stronger ice-volume forcing[143].

Atmosphere Ocean General Circulation Models (AOGCM) show a strong relationship of the monsoon with the NH insolation, which weakens with the increasing glacial boundary conditions[144], as was confirmed later[145–147]. But recent studies have shown that internal feedback mechanisms such as land conditions including albedo, soil moisture, vegetation via change in albedo and transpiration[148–152], SST variability in oceans (e.g., delays the retreat of monsoon via late summer warming[153,154]) modulate the insolation effects. Additional ocean feedback mechanism was invoked to explain how intense monsoon rainfall early in the season can cause stratification in the Bay of Bengal, reducing the mixed layer depth, thus altering the thermal inertia of the surface ocean. In such a case, both the ocean response and the insolation forcing are in phase[155]. ENSO exerts significant control over the monsoon system and several studies have tried to explore the effect of earth's orbital variability on ENSO. Clement *et al.*[156], using a simplified AOGCM, found that orbital variability certainly modulates the ENSO, e.g. during the mid-Holocene the strong ENSO events were fewer and the mean amplitude power, than the present. On the other hand, fully coupled AOGCM showed that there was no change in ENSO variability during the mid-Holocene[157], whereas it reduced during the early Holocene[158]. In short, modelling results show that monsoon variability is governed not only by orbital parameters and glacial boundary conditions but also by any factor that affects the inter-hemispheric pressure/wind gradients, moisture flux and SST.

1. Tiwari, M., Managave, S., Yadava, M. G. and Ramesh, R., Spatial and temporal coherence of paleomonsoon records from marine and land proxies in the Indian region during the past 30 ka. *J. Earth Syst. Sci.*, 2010, **119**, 197–215.
2. Kumar, K. K., Rajagopalan, B. and Cane, M. A., On the weakening relationship between the Indian monsoon and ENSO. *Science*, 1999, **284**, 2156–2159.
3. Goswami, B. N., Venugopal, V., Sengupta, D., Madhusoodan, M. S. and Xavier, P., Increasing trend of extreme rain events over India in a warming environment. *Nature*, 2006, **314**, 1442–1445.
4. Mayewski, P. A. *et al.*, Changes in atmospheric circulation and ocean ice cover over the North Atlantic during the last 41,000 years. *Science*, 1994, **263**, 1747–1751.
5. Walker, M. *et al.*, Formal definition and dating of the gssp (global stratotype section and point) for the base of the Holocene using the Greenland NGRIP ice core, and selected auxiliary records. *J. Quaternary Sci.*, 2009, **24**(1), 3–17.
6. Lowe, J. J. and Walker, M., *Reconstructing Quaternary Environments*, Addison-Wesley, London, 1997, 2nd edn.
7. Fritts, H. C., *Tree Rings and Climate*, Academic Press, 1976.
8. Managave, S. R. and Ramesh, R., Isotope dendroclimatology: a review with a special emphasis on tropics. In *Handbook of Environmental Isotope Geochemistry* (ed. Baskaran, M.), 2011 (in press).
9. Ramesh, R., Bhattacharya, S. K. and Gopalan, K., Dendroclimatological implications of isotope coherence in trees from Kashmir Valley, India. *Nature*, 1985, **317**, 802–804.
10. Borgaonkar, H. P., Sikder, A. B., Somaru Ram, Rupa Kumar, K. and Pant, G. B., Dendroclimatological investigations of high altitude Himalayan conifers and tropical teak in India. *Kor. J. Quaternary Res.*, 2007, **21**, 15–25.
11. Shah, S. K., Bhattacharyyaa, A. and Chaudhary, V., Reconstruction of June–September precipitation based on tree-ring data of teak (*Tectona grandis* L.) from Hoshangabad, Madhya Pradesh, India. *Dendrochronologia*, 2007, **25**, 57–64.
12. Hughes, M. K., Dendroclimatic evidence from the western Himalaya. In *Climate Since AD 1500* (eds Bradley, R. S. and Jones, P. D.), London, Routledge, 1992, pp. 415–431.
13. Yadav, R. R. and Singh, J., Tree-ring-based spring temperature patterns over the past four centuries in Western Himalaya. *Quaternary Res.*, 2002, **57**, 299–305.
14. Sano, M., Sheshshayee, M. S., Managave, S., Ramesh, R., Sukumar, R. and Sweda, T., Climatic potential of $\delta^{18}O$ of *Abies*

spectabilis from the Nepal Himalaya. *Dendrochronologia*, 2010, **28**, 93–98.
15. Yadava, M. G. and Ramesh, R. R., Monsoon reconstruction from radiocarbon dated tropical speleothems. *The Holocene*, 2005, **15**, 48–59.
16. Managave, S. R., Sheshshayee, M. S., Ramesh, R., Borgaonkar, H. P., Shah, S. K. and Bhattacharyya, A., Response of cellulose oxygen isotope values of teak trees in differing monsoon environments to monsoon rainfall. *Dendrochronologia*, 2011 (in press).
17. Bhattacharyya, A., Yadav, R. R., Borgaonkar, H. P. and Pant, G. B., Growth-ring analysis of Indian tropical trees: dendroclimatic potential. *Curr. Sci.*, 1992, **62**(11), 736–741.
18. Ram, S., Borgaonkar, H. P. and Sikder, A. B., Tree-ring analysis of teak (*Tectona grandis* L.F.) in central India and its relationship with rainfall and moisture index. *J. Earth Syst. Sci.*, 2008, **117**, 637–645.
19. Cook, E. R., Anchukaitis, K. J., Buckley, B. M., D'Arrigo, R. D., Jacoby, G. C. and Wright, W. E., Asian monsoon failure and megadrought during the last millennium. *Science*, 2010, **328**, 486–489.
20. Borgaonkar, H. P., Sikder, A. B., Ram Somaru and Pant, G. B., El Niño and related monsoon drought signals in 523-year-long ring width records of teak (*Tectona grandis* L.F.) trees from south India. *Palaeogeogr., Palaeoclimatol., Palaeoecol.*, 2010, **285**, 74–84.
21. Bhattacharyya, A., Eckstein, D., Shah, S. K. and Chaudhary, V., Analyses of climatic changes around Perambikulum, South India, based on early wood mean vessel area of teak. *Curr. Sci.*, 2007, **93**, 1159–1164.
22. Singh, J., Yadav, R. R., Dubey, B. and Chaturvedi, R., Millennium-long ring-width chronology of Himalayan cedar from Garhwal Himalaya and its potential in climate change studies. *Curr. Sci.*, 2004, **86**(4), 590–593.
23. Yadav, R. R., Singh, J., Dubey, B. and Misra, K. G., A 1584-year ring width chronology of juniper from Lahul, Himachal Pradesh: Prospects of developing millennia-long climate records. *Curr. Sci.*, 2006, **90**(8), 1122–1126.
24. Singh, J. and Yadav, R. R., Dendroclimatic potential of millennium-long ring-width chronology of *Pinus gerardiana* from Himachal Pradesh, India. *Curr. Sci.*, 2007, **93**, 833–836.
25. Borgaonkar, H. P., Pant, G. B. and Rupa Kumar, K., Ring-width variations in *Cedrus deodara* and its climatic response over the western Himalaya. *Int. J. Climatol.*, 1996, **16**, 1409–1422.
26. Singh, J. and Yadav, R. R., Spring precipitation variations over the western Himalaya, India, since AD 1731 as deduced from tree rings. *J. Geophys. Res.*, 2005, **110**, D01110: doi:10.1029/2004JD004855.
27. Singh, J., Park, W. K. and Yadav, R. R., Tree-ring-based hydrological records for western Himalaya, India, since AD 1560. *Clim. Dyn.*, 2006, **26**, 295–303.
28. Singh, J., Yadav, R. R. and Wilmking, M., A 694-year tree-ring based rainfall reconstruction from Himachal Pradesh, India. *Clim. Dyn.*, 2009, **33**, 1149–1158; doi: 10.1007/s00382-009-0528-5.
29. Chaudhary, V. and Bhattacharyya, A., Suitability of *Pinus kesiya* in Shillong, Meghalaya for tree-ring analyses. *Curr. Sci.*, 2002, **83**, 1010–1015.
30. Ramesh, R., Bhattacharya, S. K. and Pant, G. B., Climatic significance of δD variations in a tropical tree species from India. *Nature*, 1989, **337**, 149–150.
31. Ramesh, R., Bhattacharya, S. K. and Gopalan, K., Climatic correlations in the stable isotope records of silver fir (*Abies pindrow*) trees from Kashmir, India. *Earth Planet. Sci. Lett.*, 1986, **79**, 66–74.
32. Managave, S. R., Sheshshayee, M. S., Borgaonkar, H. P. and Ramesh, R., Past break-monsoon conditions detectable by high resolution intra-annual δ^{18}O analysis of teak rings. *Geophys. Res. Lett.*, 2010, **37**, L05702, doi:10.1029/2009GL041172.
33. Managave, S. R., Sheshshayee, M. S., Borgaonkar, H. P. and Ramesh, R., Intra-annual oxygen isotope variations in central Indian teak cellulose: possibility of improved resolution for past monsoon reconstruction. *Curr. Sci.*, 2010, **98**, 930–937.
34. Managave, S. R., Sheshshayee, M. S., Bhattacharyya, A. and Ramesh, R., Intra-annual variations of cellulose δ^{18}O of teak from Kerala, India: implications to reconstruction of past summer and winter monsoon rains. *Clim. Dyn.*, 2011 (in press).
35. Diaz, H. F. and Kiladis, G. N., Atmospheric teleconnections associated with the extreme phases of the Southern oscillation. In *El Nino, Historical and Paleoclimatic Aspects of the Southern Oscillation* (eds Diaz, H. F. and Markgraf, V.), Cambridge Univ. Press, Cambridge, 1992, pp. 7–28.
36. Felis, T., Patzold, J., Loya, Y., Fine, M., Nawar, A. H. and Wefer, G., A coral oxygen isotope record from the northern Red Sea documenting NAO, ENSO, and North Pacific teleconnections on Middle East climate variability since the year 1750. *Paleoceanography*, 2000, **15**, 679–694.
37. Shukla, J., Effect of Arabian Sea surface temperature anomaly on Indian summer monsoon: a numerical experiment with the GFDL model. *J. Atm. Sci.*, 1975, **32**, 503–511.
38. Kershaw, R., Effect of a sea surface temperature anomaly on a prediction of the onset of the southwest monsoon over India. *Quart. J. R. Meteorol. Soc.*, 1988, **114**, 325–345.
39. Yang, S. and Lau, K. M., Influences of sea surface temperature and ground wetness on the Asian summer monsoon. *J. Climatol.*, 1998, **11**, 3230–3246.
40. Chakraborty, S. and Ramesh, R., Stable isotope variations in a coral (*Favia speciosa*) from the Gulf of Kutch during 1948–1989 AD: environmental implications. *Proc. Indian Acad. Sci. (Earth. Planet. Sci.)*, 1998, **107**, 331–341.
41. Tudhope, A. W., Lea, D. W., Shimmield, G. B., Chilcott, C. P. and Head, S., Monsoon climate and Arabian Sea coastal upwelling recorded in massive corals from Southern Oman. *Palaios*, 1996, **11**, 347–361.
42. Klein, R. *et al.*, Evaluating southern Red Sea corals as a proxy record for the Asian monsoon. *Earth Planet. Sci. Lett.*, 1997, **148**, 381–394.
43. Chakraborty, S. and Ramesh, R., Environmental significance of carbon and oxygen isotope ratios of banded corals from Lakshadweep, India. *Quaternary Int.*, 1997, **37**, 55–65.
44. Ahmad, M. *et al.*, High-resolution carbon and oxygen isotope records from a scleractinian (*Porites*) coral of Lakshadweep Archipelago. *Quaternary Int.*, 2010 (in press).
45. Chakraborty, S. and Ramesh, R., Monsoon induced sea surface temperature changes recorded in Indian corals. *Terra Nova*, 1993, **5**, 545–551.
46. Charles, C. D., Hunter, D. E. and Fairbanks, R. G., Interaction between the ENSO and the Asian monsoon in a coral record of tropical climate. *Science*, 1997, **277**, 925–928.
47. Pfeiffer, M. and Dullo, W. C., Monsoon-induced cooling of the western equatorial Indian Ocean as recorded in coral oxygen isotope records from the Seychelles covering the period of 1840–1994 AD. *Quat. Sci. Rev.*, 2006, **25**, 993–1009.
48. Cole, J. E., Dunbar, R. B., McClanahan, T. R. and Muthiga, N., Tropical Pacific forcing of decadal variability in the western Indian Ocean over the past two centuries. *Science*, 2000, **287**, 617–619.
49. Webster, P. J. *et al.*, Monsoons: processes, predictability, and the prospects for prediction. *J. Geophys. Res.*, 1998, **103**, 14451–14510.
50. Vinayachandran, P. N., Summer cooling of the Arabian Sea during contrasting monsoons. *Geophys. Res. Lett.*, 2004, **31**, L13306.
51. Pfeiffer, M., Timm, O. and Dullo, W.-C., Oceanic forcing of interannual and multidecadal climate variability in the southwestern Indian Ocean: evidence from a 160 year coral isotopic

record (La Réunion, 55°E, 21°S). *Paleoceanography*, 2004, **19**; doi:10.1029/2003PA000964.
52. Timm, O., Pfeiffer, M. and Dullo, W., Nonstationary ENSO-precipitation teleconnection over the equatorial Indian Ocean documented in a coral from the Chagos Archipelago. *Geophys. Res. Lett.*, 2005, **32**, L02701, doi:10.1029/2004GL021738.
53. Ramanathan, V. and Collins, W., Thermodynamic regulation of ocean warming by cirrus clouds deduced from observations of the 1987 El Nino. *Nature*, 1991, **351**, 27–32.
54. Lindzen, R. S., Chou, M.-D. and Hou, A. Y., Does the Earth have an adaptive infrared iris? *Bull. Am. Meteorol. Soc.*, 2001, **82**, 417–432.
55. Zinke, J. and the KIHZ Consortium, evidence for the climate during the Late Maunder minimum from proxy data and model simulations available within KIHZ. In *The Climate in Historical Times – Towards a Synthesis of Holocene Proxy Data and Climate Models* (eds von Storch, H., Raschke, E. and Floeser, G.), Springer, 2004, pp. 397–414.
56. Zinke, J., Dullo, W.-C., Heiss, G. A. and Eisenhauer, A., ENSO and Indian Ocean subtropical dipole variability is recorded in a coral record off southwest Madagascar for the period 1659–1995. *Earth Planet. Sci. Lett.*, 2004, **228**, 177–197.
57. Zinke, J., Pfeiffer, M., Timm, O., Dullo, W. C. and Davies, G. R., Atmosphere-ocean dynamics in the Western Indian Ocean recorded in corals. *Philos. Trans. R. Soc. A*, 2005, **363**, 121–142.
58. Saji, N. H., Goswami, B. N., Vinayachandran, P. N. and Yamagata, T., A dipole mode in the tropical Indian Ocean. *Nature*, 1999, **401**, 360–363.
59. Abram, N. J., Gagan, M. K., Cole, J. E., Hantoro, W. S. and Mudelsee, M., Recent intensification of tropical climate variability in the Indian Ocean. *Nature Geosci.*, 2008, **1**, 849–853; doi: 10.1038/ngeo357.
60. Charles, C. D., Cobb, K. M., Moore, M. D. and Fairbanks, R. G., Monsoon–tropical ocean interaction in a network of coral records spanning the 20th century. *Mar. Geol.*, 2003, **201**, 207–222.
61. Abram, N. J., Gagan, M. K., Liu, Z., Hantoro, W. S., McCulloch, M. T. and Suwargadi, B. W., Seasonal characteristics of the Indian Ocean Dipole during the Holocene epoch. *Nature*, 2007, **445**; doi:10.1038.
62. Thompson, L. G. *et al.*, Tropical climate instability: the last glacial cycle from a Qinghai–Tibetan ice core. *Science*, 1997, **276**, 1821–1825.
63. Thompson, L. G. *et al.*, 100,000 year climate record from Qinghai–Tibetan Plateau ice cores. *Science*, 1989, **246**(4929), 474–477.
64. Thompson, L. G., Mosley-Thompson, E., Davis, M. E., Lin, P.-N., Henderson, K. and Mashiotta, T. A., Tropical glacier and ice core evidence of climate change on annual to millennial time scales. *Climatic Change*, 2003, **59**, 137–155.
65. Thompson, L. G., Yao, T., Mosley-Thompson, E., Davis, M. E., Henderson, K. A. and Lin, P.-N., A high-resolution millennial record of the South Asian Monsoon from Himalayan ice cores. *Science*, 2000, **289**, 1916–1919.
66. Thompson, L. G., Mosley-Thompson, E., Davis, M. E., Lin, P.-N., Henderson, K. and Mashiotta, T. A., Tropical glacier and ice core evidence of climate change on annual to millennial time scales. *Climatic Change*, 2003, **59**, 137–155.
67. Yang, B., Braeunung, A., Yao, T. and Davis, M. E., Correlation between the oxygen isotopic record from Dasuopu ice core and the Asian Southwest Monsoon during the last millennium. *Quat. Sci. Rev.*, 2007, **26**, 1810–1817.
68. Ford, D., Paleoenvironments: speleothems. In *Encyclopedia of Caves and Karst Science* (ed. Gunn, J.), Fitzroy Dearborn, New York, 2004.
69. Yadava, M. G. and Ramesh, R., Speleothems – useful proxies for past monsoon rainfall. *J. Sci. Ind. Res.*, 1999, **58**, 339–348.
70. Yadava, M. G. and Ramesh, R., Monsoon reconstruction from radiocarbon dated tropical Indian speleothems. *The Holocene*, 2005, **15**(1), 50–62.
71. Yadava, M. G., Ramesh, R., Polyak, V. J. and Asmerom, Y., Age spans of some Indian speleothems. Proceedings of the 11th ISMAS-TRICON-2009, Hyderabad, 24–28 November 2009.
72. Yadava, M. G., Saraswat, K. S., Singh, I. B. and Ramesh, R., Evidences of the early human occupation in the limestone caves of Bastar, Chhattisgarh. *Curr. Sci.*, 2007, **92**(6), 820–823.
73. Yadava, M. G., Ramesh, R., Asmerom, Y. and Polyak, V. J., Holocene increase in the Bay Branch of the monsoon inferred from $\delta^{18}O$ of speleothems from Central India, Abstr., AGU Fall Meeting, San Francisco, 15–19 December 2008.
74. Yadava, M. G. and Ramesh, R., Past rainfall and trace element variations in a tropical speleothem from India. *Mausam*, 2001, **52**, 307–316.
75. Sinha, A. *et al.*, A 900-year (600 to 1500 AD) record of the Indian summer monsoon precipitation from the core monsoon zone of India. *Geophys. Res. Lett.*, 2007, **34**, L16707; doi:10.1029/2007GL030431.
76. Yadava, M. G., Ramesh, R. and Pant, G. B., Past monsoon rainfall variations in peninsular India recorded in a 331 year old speleothem. *The Holocene*, 2004, **14**(4), 517–524.
77. Yadava, M. G. and Ramesh, R., Significant longer-term periodicities in the proxy record of the Indian monsoon rainfall. *New Astron.*, 2007, **12**, 544–555.
78. Yadava, M. G. and Ramesh, R., Decadal variability in the Indo-Gangetic monsoon rainfall during the last ~2800 years: Speleothem $\delta^{18}O$ evidence from the Sota cave, Uttar Pradesh. In *Antarctic Geoscience, Ocean–Atmosphere Interaction and Paleoclimatology* (eds Rajan, S. and Pandey, P. C.), NCAOR, Goa, 2005, pp. 185–197.
79. Yadava, M. G. and Ramesh, R., Stable oxygen and carbon isotope variations as monsoon proxies: a comparative study of speleothems from four different locations in India. *J. Geol. Soc. India*, 2006, **68**, 461–475.
80. Sinha, A. *et al.*, Variability of Southwest Indian summer monsoon precipitation during the Bølling-Ållerød. *Geology*, 2005, **33**, 2005, 813.
81. Yadava, M. G., Ramesh, R. and Pandarinath, K., A positive 'amount effect' in the Sahyadri (Western Ghats) rainfall. *Curr. Sci.*, 2007, **93**(2), 560–564.
82. Dansgaard, W., Stable isotopes in precipitation. *Tellus*, 1964, **16**, 436–468.
83. Ivanochko, T. S., Ganeshram, R. S., Brummer, G. J. A., Ganssen, G., Jung, S. J. A., Moreton, S. G. and Kroon, D., Variations in tropical convection as an amplifier of global climate change at the millennial scale. *Earth Planet. Sci. Lett.*, 2005, **235**, 302–314.
84. Shi, W., Morrison, J. M., Bohm, E. and Manghnani, V., The Oman upwelling zone during 1993, 1994 and 1995. *Deep Sea Res. II*, 2000, **47**, 1227–1247.
85. Sarkar, A., Ramesh, R., Somayajulu, B. L. K., Agnihotri, R., Jull, A. J. T. and Burr, G. S., High resolution Holocene monsoon record from the eastern Arabian Sea. *Earth Planet. Sci. Lett.*, 2000, **177**, 209–218.
86. Govil, P. and Naidu, P. D., Evaporation–precipitation changes in the eastern Arabian Sea for the last 68 ka: Implications on monsoon variability. *Paleoceanography*, 2010, **25**, PA1210; doi:10.1029/2008PA001687.
87. Shetye, S. R., Seasonal variability of the temperature field off the southwest coast of India. *Proc. Indian Acad. Sci.*, 1994, **93**(4), 399–411.
88. Sirocko, F., Sarnthein, M., Erlenkreuser, H., Lange, H., Arnold, M. and Duplessy, J. C., Century scale events in monsoon climate over the past 24,000 years. *Nature*, 1993, **364**, 322–324.

89. Overpeck, J., Anderson, D., Trumbore, S. and Prell, W., The southwest Indian Monsoon over the last 18000 years. *Clim. Dynam.*, 1996, **12**, 213–225.
90. Anderson, D. M. and Prell, W. L., A 300 kyr record of upwelling off Oman during the Late Quaternary: evidence of the Asian Southwest monsoon. *Paleoceanography*, 1993, **8**, 193–208.
91. Naidu, P. D. and Malmgren, B. A., A high-resolution record of late Quaternary upwelling along the Oman margin, Arabian Sea based on planktonic foraminifera. *Paleoceanography*, 1996, **11**, 129–140.
92. Gupta, A. K., Anderson, D. M. and Overpeck, J. T., Abrupt changes in the Asian southwest monsoon during the Holocene and their links to the North Atlantic Ocean. *Nature*, 2003, **421**, 354–357.
93. Gupta, A. K., Das, M. and Anderson, D. M., Solar influence on the Indian summer monsoon during the Holocene. *Geophys. Res. Lett.*, 2005, **32**, L17703; doi:10.1029/2005GL022685.
94. Berger, A., Orbital variations and insolation database. IGBP PAGES/World Data Center for Paleoclimatology Data Contribution Series # 92–007. NOAA/NGDC Paleoclimatology Program, Boulder CO, USA, 1992.
95. Anderson, D. M., Baulcomb, C. K., Duvuvuer, A. K. and Gupta, A. K., Indian summer monsoon during the last two millennia. *J. Quat. Sci.*, 2010, **25**(6), 911–917.
96. Wyrtki, K., *Oceanographic Atlas of the International Indian Ocean Expedition*, National Science Foundation Publication, OCE/NSF 86-00-001, Washington DC, 1971, p. 531.
97. Reichart, G. J., Dulk, M. D., Visser, H. J., van der Weijden, C. H. and Zachariasse, W. J., A 225 kyr record of dust supply, paleoproductivity and the oxygen minimum zone from the Murray Ridge (northern Arabian Sea). *Palaeogeor., Palaeoclimatol., Palaeoecol.*, 1997, **134**, 149–169.
98. Reichart, G. J., Lourens, L. J. and Zachariasse, W. J., Temporal variability in the Northern Arabian Sea Oxygen Minimum Zone (OMZ) during the last 225,000 years. *Paleoceanography*, 1998, **13**, 607–621.
99. Ganeshram, R. S., Pederson, T. F., Calvert, S. E. and François, R., Reduced nitrogen fixation in the glacial ocean inferred from changes in marine nitrogen and phosphorus inventories. *Nature*, 2002, **415**, 156–159.
100. Altabet, M. A., Higginson, M. J. and Murray, D. W., The effect of millennial – scale changes in Arabian Sea denitrification on atmospheric CO_2. *Nature*, 2002, **415**, 159–162.
101. Saher, M. H. *et al.*, Western Arabian Sea SST during the penultimate interglacial: A comparison of $U^{K'}_{37}$ and Mg/Ca paleothermometry. *Paleoceanography*, 2009, **24**, PA2212; doi:10.1029/2007PA001557.
102. Naidu, P. D. and Malmgren, B. A., Seasonal sea surface temperature contrast between the Holocene and last glacial period in the western Arabian Sea (Ocean Drilling Project Site 723A): Modulated by monsoon upwelling. *Paleoceanography*, 2005, **20**, PA1004; doi:10.1029/2004PA001078.
103. Anand, P., Kroon, D., Singh, A. D., Ganeshram, R. S., Ganssen, G. and Elderfield, H., Coupled sea surface temperature–seawater $\delta^{18}O$ reconstructions in the Arabian Sea at the millennial scale for the last 35 ka. *Paleoceanography*, 2008, **23**, PA4207; doi: 10.1029/2007PA001564.
104. Staubwasser, M., Sirocko, F., Grootes, P. M. and Segl, M., Climate change at the 4.2 ka BP termination of the Indus valley civilization and Holocene south Asian monsoon variability. *Geophys. Res. Lett.*, 2003, **30**, 1425–1428.
105. Rostek, F., Ruhland, G., Bassinot, F. C., Muller, P. J., Labeyrie, L. D., Lancelot, Y. and Bard, E., Reconstructing sea surface temperature and salinity using $\delta^{18}O$ and alkenone records. *Nature*, 1993, **364**, 319–321.
106. Saraswat, R., Nigam, R., Weldeab, S., Mackensen, A. and Naidu, P. D., A first look at past sea surface temperatures in the equatorial Indian Ocean from Mg/Ca in foraminifera. *Geophys. Res. Lett.*, 2005, **32**, L24605.
107. Tiwari, M., Ramesh, R., Somayajulu, B. L. K., Jull, A. J. T. and Burr, G. S., Paleomonsoon precipitation deduced from a sediment core from the equatorial Indian Ocean. *Geo-Marine Lett.*, 2006, **26**, 23–30; doi: 10.1007/s00367-005-0012-0.
108. Thamban, M., Rao, V. P., Schneider, R. R. and Grootes, P. M., Glacial to Holocene fluctuations in hydrography and productivity along the southwestern continental margin of India. *Palaeogeogr., Palaeoclimatol., Palaeoecol.*, 2001, **165**, 113–127.
109. Agnihotri, R., Bhattacharya, S. K., Sarin, M. M. and Somayajulu, B. L. K., Changes in the surface productivity and subsurface denitrification during the Holocene: A multiproxy study from the eastern Arabian Sea. *The Holocene*, 2003, **13**, 701–713.
110. Tiwari, M. *et al.*, Did the Indo-Asian summer monsoon decrease during the Holocene following insolation? *J. Quaternary Sci.*, 2010, **25**, 1179–1188; doi:10.1002/jqs.1398.
111. Haake, B., Rixen, T. and Ittekkot, V., Variability of monsoonal upwelling signals in the deep western Arabian Sea. In *Monsoon Biogeochemistry* (eds Ittekkot, V. and Nair, R. R.), Mitt. Geol. Palaontol. Inst. Univ., Hamburg, 1993, vol. 76, pp. 85–96.
112. Morrison, J., Codispoti, L. A., Gaurin, S., Jones, B., Manghnani, V. and Zheng, Z., Seasonal variation of hydrographic and nutrient fields during the US JGOFS Arabian Sea Process Study. *Deep-Sea Res. II*, 1998, **45**, 2053–2101.
113. Rixen, T., Haake, B. and Ittekkot, V., Sedimentation in the western Arabian Sea the role of coastal and open-ocean upwelling. *Deep-Sea Res. II*, 2000, **47**, 2155–2178.
114. Brock, J. C., McClain, C. R. and Hay, W. W., A southwest monsoon hydrographic climatology for the northwestern Arabian Sea. *J. Geophys. Res.*, 1992, **97**, 9455–9465.
115. Rixen, T., Haake-Gaye, B., Ittekkot, V., Guptha, M. V. S., Nair, R. R. and Schlussel, P., Coupling between SW monsoon-related surface and deep ocean processes as discerned from continuous particle flux measurements and correlated satellite data. *J. Geophys. Res.*, 1996, **101**, 28569–28582.
116. Brock, J. C., McClain, C. R., Luther, M. E. and Hay, W. W., The phytoplankton bloom in the northwestern Arabian Sea during the southwest monsoon of 1979. *J. Geophys. Res.*, 1991, **96**, 20613–20622.
117. Naidu, P. D., Malmgren, B. A. and Bornmalm, L., Quaternary history of the calcium carbonate fluctuations in the western equatorial Indian Ocean (Somali basin). *Palaeogeor., Palaeoclimatol., Palaeoecol.*, 1993, **103**, 21–30.
118. Murray, D. W. and Prell, W. L., Pliocene to Pleistocene variations in calcium carbonate, organic carbon and opal on the Owen Ridge, northern Arabian Sea. *Proc. ODP Sci. Results*, 1991, **117**, 343–355.
119. Clemens, S. C. and Prell, W., Non-stationary phase of the Plio-Pleistocene Asian Monsoon. *Science*, 1996, **274**, 943–948.
120. Clemens, S. C. and Prell, W., A 350,000 year summer–monsoon multiproxy stack from the Owen Ridge, Northern Arabian Sea. *Mar. Geol.*, 2003, **201**, 35–51.
121. Clemens, S. C. and Prell, W., The timing of orbital-scale Indian monsoon changes. *Quat. Sci. Rev.*, 2007, **26**, 275–278.
122. Duplessy, J. C., Glacial to interglacial contrasts in the northern Indian Ocean. *Nature*, 1982, **295**, 494–498.
123. Chauhan, O. S. and Suneethi, J., 18 ka BP records of climatic changes, Bay of Bengal: Isotopic and sedimentological evidences. *Curr. Sci.*, 2001, **81**, 1231–1234.
124. Chauhan, O. S., Past 20,000-year history of Himalayan aridity: Evidenced from oxygen isotope records in the Bay of Bengal. *Curr. Sci.*, 2003, **84**, 90–93.
125. Ahmad, S. M., Babu, G. A., Padmakumari, V. M. and Raza, W., Surface and deep water changes in the northeast Indian Ocean during the last 60 ka inferred from carbon and oxygen isotopes of planktic and benthic foraminifera. *Palaeogeogr., Palaeoclimatol., Palaeoecol.*, 2008, **262**, 182–188.

126. Kudrass, H. R., Hofmann, A., Doose, H., Emeis, K. and Erlenkeuser, H., Modulation and amplification of climate changes in Northern Hemisphere by Indian summer monsoon during the past 80 kyr. *Geology*, 2001, **29**, 63–66.
127. Cullen, J. L., Microfossil evidence for changing salinity patterns in the Bay of Bengal over the last 20,000 years. *Palaeogeogr. Palaeoclimatol. Palaeoecol.*, 1981, **35**, 315–356.
128. Rashid, H., Flower, B. P., Poore, R. Z. and Quinn, T. M., A ~25 ka Indian Ocean monsoon variability record from the Andaman Sea. *Quaternary Sci. Rev.*, 2007, **26**, 2586–2597.
129. Morrill, C., Overpeck, J. T. and Cole, J. E., A synthesis of abrupt changes in the Asian summer monsoon since the last deglaciation. *The Holocene*, 2003, **13**, 465–476.
130. Tiwari, M., Ramesh, R., Yadava, M. G., Somayajulu, B. L. K., Jull, A. J. T. and Burr, G. S., Is there a persistent control of monsoon winds by precipitation during the late Holocene. *Geochem. Geophys. Geosys.*, 2006, **7**, Q03001; doi:10.1029/2005GC001095.
131. von Rad, U., Schaaf, M., Michels, K. H., Schulz, H., Berger, W. H. and Sirocko, F., A 5000-yr record of climate change in varved sediments from the oxygen minimum zone off Pakistan, Northeastern Arabian Sea. *Quaternary Res.*, 1999, **51**, 39–53.
132. Lückge, A., Doose-Rolinski, A., Khan, A. A., Schulz, H. and von Rad, U., Monsoonal variability in the northeastern Arabian Sea during the past 5000 years: Geochemical evidence from laminated sediments. *Palaeogeogr., Palaeoclimatol., Palaeoecol.*, 2001, **167**, 273–286.
133. Chauhan, O. S., Vogelsang, E., Basavaiah, N. and Kader, U. S. A., Reconstruction of the variability of the southwest monsoon during the past 3 ka, from the continental margin of the southeastern Arabian Sea. *J. Quaternary Sci.*, 2009, **25**, 798–807; doi: 10.1002/jqs.1359,1–10.
134. Agnihotri, R., Dutta, K., Bhushan, R. and Somayajulu, B. L. K., Evidence for solar forcing on the Indian monsoon during the last millennium. *Earth Planet. Sci. Lett.*, 2002, **198**, 521–527.
135. Tiwari, M., Ramesh, R., Somayajulu, B. L. K., Jull, A. J. T. and Burr, G. S., Early Deglacial (~19–17 ka) strengthening of the Northeast monsoon. *Geophys. Res. Lett.*, 2005, **32**, L19712; doi: 10.1029/2005GL024070.
136. Thamban, M., Kawahata, H. and Rao, V. P., Indian summer monsoon variability during the Holocene as recorded in sediments of the Arabian Sea: Timing and implications. *J. Oceanogr.*, 2007, **63**, 1009–1020.
137. Tiwari, M. and Ramesh, R., Solar variability in the past and paleoclimate data pertaining to the Southwest monsoon. *Curr. Sci.*, 2007, **93**, 477–487.
138. Jagadheesha, D., Nanjundaiah, R. and Ramesh, R., Orbital forcing of Monsoonal climates in NCAR CCM2 with two horizontal resolutions. *Palaeoclimates – Data and Modelling*, 1999, **3**, 279–301.
139. Kutzbach, J. E., Monsoon climate of the early Holocene: Climate experiment with the Earth's orbital parameters for 9000 years ago. *Science*, 1981, **214**, 59–61.
140. Schulz, H., von Rad, U. and Erlenkeuser, H., Correlation between Arabian Sea and Greenland climate oscillations of the past 110,000 years. *Nature*, 1998, **393**, 54–57.
141. Wang, P. *et al.*, Evolution and variability of the Asian monsoon system: state of the art and outstanding issues. *Quaternary Sci. Rev.*, 2005, **24**, 595–629.
142. Clemens, S. C., Prell, W., Murray, D., Shimmield, G. and Weedon, G., Forcing mechanisms of the Indian Ocean monsoon. *Nature*, 1991, **353**, 720–725.
143. Emeis, K.-C., Anderson, D. M., Doose, H., Kroon, D. and Schulz-Bull, D., Sea-surface temperatures and the history of monsoon upwelling in the northwest Arabian Sea during the last 500,000 years. *Quaternary Res.*, 1995, **43**, 355–361.
144. Prell, W. L. and Kutzbach, J. E., Monsoon variability over the past 150,000 years. *J. Geophys. Res.*, 1987, **92**, 8411–8425.
145. Wright Jr, H. T., Kutzbach, J. E., Webb III, T., Ruddiman, W. E. F., Street-Perrott, F. A. and Bartlein, P. J. (eds), *Global Climates Since the Last Glacial Maximum*, University of Minnesota Press, Milleapolis, 1993, p. 569.
146. de Noblet, N., Braconnot, P., Joussaume, S. and Masson, V., Sensitivity of simulated Asian and African summer monsoons to orbitally induced variations in insolation 126, 115 and 6 kBP. *Clim. Dynam.*, 1996, **12**, 589–603.
147. Dong, B., Valdes, P. J. and Hall, N. M. J., The changes of monsoonal climates due to Earth's orbital perturbations and ice age boundary conditions. *Paleoclimates – Data and Modelling*, 1996, **1**, 203–240.
148. Street-Perrott, F. A., Mitchell, J. F. B., Marchand, D. S. and Btunner, J. S., Milankovitch and albedo forcing of the tropical monsoons: a comparison of geological evidence and numerical simulations for 9000 yr BP. *Trans. R. Soc. Edinburgh: Earth Sci.*, 1990, **81**, 407–427.
149. Bonfils, C., de Noblet-Ducoudré, N., Braconnot, P. and Joussaume, J., Desert albedo and climate change: mid-Holocene monsoon in North Africa. *J. Climate*, 2001, **14**, 3724–3737.
150. Kutzbach, J., Bonan, G., Foley, J. and Harrison, S. P., Vegetation and soil feedbacks on the response of the African monsoon to orbital forcing in the early to middle Holocene. *Nature*, 1996, **384**, 623–626.
151. Claussen, M. and Gayler, V., The greening of the Sahara during the mid-Holocene: results of an interactive atmosphere-biome model. *Global Ecol. Biogeogr. Lett.*, 1997, **6**, 369–377.
152. Doherty, R., Kutzbach, J., Foley, J. and Pollard, D., Fully coupled climate/dynamical vegetation model simulations over Northern Africa during the mid-Holocene. *Clim. Dynam.*, 2000, **16**, 561–573.
153. Hewitt, C. D. and Mitchell, J. F. B., A fully coupled GCM simulation of the climate of the mid-Holocene. *Geophys. Res. Lett.*, 1998, **25**, 361–364.
154. Braconnot, P., Marti, O., Joussaume, S. and Leclainche, Y., Ocean feedback in response to 6 kyr Before Present insolation. *J. Climate*, 2000, **13**, 1537–1553.
155. Braconnot, P. and Marti, O., Impact of precession on monsoon characteristics from coupled ocean atmosphere experiments: changes in Indian monsoon and Indian Ocean climatology. *Mar. Geol.*, 2003, **201**, 23–34.
156. Clement, A. C., Seager, R. and Cane, M. A., Orbital controls on the El Nino/Southern Oscillation and the tropical climate. *Paleoceanography*, 1999, **14**, 441–456.
157. Otto-Bliesner, B. L., El Niño/La Niña and Sahel precipitation during the middle Holocene. *Geophys. Res. Lett.*, 1999, **26**, 87–90.
158. Liu, Z., Jacob, R., Kutzbach, J., Wu, L., Anderson, J. and Harrison, S., Monsoon impact on El-Niño in the Early Holocene. In Paleoclimate Modeling Intercomparison Project (PMIP) (ed. Braconnot, P.), Proceedings of the Third PMIP Workshop, 2000, pp. 205–209.
159. Yadav, R. R., Tree ring imprints of long-term changes in climate in western Himalaya, India. *J. Biosci.*, 2009, **34**(5), 699–707.

ACKNOWLEDGEMENTS. We thank C. P. Rajendran for inviting this review, Dr C. B. S. Dutt, NRSC, Hyderabad and ISRO-GBP for funding support. We thank the Directors of IITM, Pune and NCAOR, Goa, for encouragement; M. S. Srinivasan, K. Gopalan and R. Nigam for comments that improved the manuscript. We also thank R. A. Jani (PRL), M. S. Sheshshayee and Nagabhushana (UAS) and A. K. Singh (DU) for laboratory help. D.K.S. thanks Delhi University. We dedicate this review to the late B. H. Subbaraya. This is NCAOR contribution no. 043/2010.